---

**Kay, A.L.**; **Jones, D.A.**. 2012 Transient changes in flood frequency and timing in Britain under potential projections of climate change. *International Journal of Climatology*, 32 (4). 489-502. 10.1002/joc.2288

# Transient changes in flood frequency and timing in Britain under potential projections of climate change

Kay, A.L. and Jones, D.A.

Centre for Ecology and Hydrology, Maclean Building, Crowmarsh Gifford, Wallingford, Oxfordshire, OX10 8BB, UK

Correspondence to: A.L. Kay (alkay@ceh.ac.uk)

## Abstract

Climate change could have dramatic consequences for the earth's environment, especially its hydrology, yet the 'noise' of natural climate variability can mask the impacts of climate change on shorter time-scales, and can act (in an unpredictable way) to enhance or reduce its effect in any given period in the future. Thus impact studies based on time-slices, which look at modelled differences between baseline (e.g. 1961-1990) and future (e.g. 2070-2099) periods, can be misleading. This paper makes use of three new transient climate projections, from a perturbed parameter ensemble of a regional climate model (RCM) covering the period 1950-2099, to investigate transient changes in flood frequency and timing for two example catchments in England. Annual maximum (AM) time-series are extracted from modelled flow time-series (for hourly, daily-mean and running 30-day mean flows). The AM series are analysed in terms of flood frequency (using a fitted generalised logistic distribution) and timing in a 30-year moving window. A non-linear trend analysis is performed on the derived time-series, with permutation testing to estimate statistical significance. The results show that changes over the period are often non-linear, and vary considerably in size and statistical significance according to catchment, flow time-step and RCM ensemble member. The relative effects of the three RCM ensemble members are consistent with their relative climate sensitivities. A nationwide analysis, using daily mean flows from a grid-based runoff and routing model for the UK with one of the RCM ensemble members, was consistent with the catchment results in terms of direction of trends, but generally gave trends of a higher magnitude, indicating the presence of some hydrological model structure uncertainty. The nationwide results suggest increased flood risk across much of the country.

## Keywords
Transient climate change; uncertainty; hydrological impacts; annual maxima; flood frequency.

## 1. Introduction

There is a growing realisation that climate change could have important and varied environmental consequences, particularly for our hydrological cycle. However, in relatively short observational records such as river flows it is generally difficult to distinguish the effects of climate change from those of natural climate variability (Kunzewicz and Robson 2004, Hannaford and Marsh 2007, Robson 2002). Natural variability is perhaps an underestimated feature of our climate and occurs at many different spatial- and temporal-scales, from convective storms to oceanic oscillations and from hours to decades. The most well-known examples of large spatial-scale, long time-scale phenomena are probably the multi-year variation of the El Niño Southern Oscillation and the multi-decadal variation of the North Atlantic Oscillation (Kerr 2007). The latter has previously been implicated in observed changes in winter runoff and high flows in some northern and western UK rivers (Hannaford *et al.* 2007; Hannaford and Marsh 2007). In addition, decadal-scale variations in extreme rainfall in the UK have been demonstrated for 1961-2000, which differ in different regions of the country (Fowler and Kilsby 2003). Thus understanding current natural variability, and how natural variability may itself alter under climate change, could be important for understanding and detecting the impacts of climate change on river flows. Wilby *et al.* (2008) provide a useful summary of recent studies of trends in observed rainfall and flows (and modelled future flows) over the UK, including a discussion of natural variability.

Climate models produce projections of climate for future periods, under given assumptions about future emissions of greenhouse gases. Data from global climate models (GCMs) can be used indirectly to drive hydrological models, either with some form of statistical downscaling (e.g. Dettinger *et al.* 2004) or through the application of "delta changes" (where change factors suggested by climate models are applied to a baseline of observed climate data, e.g. Prudhomme *et al.* 2002). But it is only the more recent development of higher resolution regional climate models (RCMs), nested within the lower resolution GCMs, which has enabled the more direct use of climate model data to drive hydrological models at a more appropriate scale, particularly for flood modelling and for smaller catchments (e.g. Kay *et al.* 2006a, Fowler and Kilsby 2007, Graham *et al.* 2007b, Thodsen 2007). A disadvantage of the direct use of climate model data is potential bias in the data, due to systematic errors in the models. A major advantage of direct, rather than indirect, use of climate model data is the spatial consistency of the data, and the fact that it includes the effects of natural variability (over a range of time-scales). However, the latter could also be considered a problem as it means that the simulated climate change signal is confused by the 'noise' of modelled natural variability: For a given period, the modelled natural variability may act in the same direction as climate change, thus reinforcing its apparent effect in that period, or it could act in the opposite direction to climate change, thus reducing its apparent effect in that period (Murphy *et al.* 2009 (Section 2.2); Wood 2008; Kerr 2007). Precisely the same is true of natural variability in the past climate, and will be true for the real future climate. Although some progress has recently been made in predicting the directional effect of natural variability on (large-scale) temperature over the coming decade (Smith *et al*. 2007; Keenlyside *et al.* 2008), this prediction capability does not yet extend to (small-scale) precipitation, so cannot be used to predict the directional effect of natural variability on river flows, nor can it be extended to later in the century. Kendon *et al.* (2008) discuss the effects of natural variability on regional climate model projections of precipitation extremes over Europe, and recommend large natural variability ensembles for the improved prediction of changes in such extremes.

Much of the previous hydrological climate change impacts work has been based on time-slices, where modelling has been performed for two periods, often 1961-1990 ('1970s', 'Baseline') and 2071-2100 ('2080s', 'Future'), and comparisons made between the 'Baseline and 'Future' results to suggest the impact by the 2080s on the hydrological feature under consideration. However, given the presence of natural variability, as well as the inherent non-linearity of the hydrological processes that translate rainfall into river flow, it is possible that the impact in some intervening period could be quite different; it is certainly unlikely that there will be a linear change in the impact across the period. This non-linearity is demonstrated by results of Reynard *et al.* (2004) based on change factors from UKCIP02 (Hulme *et al.* 2002), where several catchments showed modelled flood frequency changes for the 2050s that were of the opposite sign to those modelled for the 2080s. This occurred despite the fact that the UKCIP02 scenarios for the 2050s were pattern-scaled from the ensemble mean of those modelled for the 2080s (that is, the regional patterns of change modelled for the 2080s were scaled back to the 2050s using modelled global-average temperature changes; Hulme *et al.* 2002, Section 3.3), thus removing the effect of natural variability between time-slices.

This paper makes use of three new transient climate projections for the period 1950-2099, produced by the UK Met Office Hadley Centre to guide the development of the latest set of climate scenarios for the UK Climate Impacts Programme (UKCP09; Murphy *et al.* 2009). These projections are used to investigate transient changes in flood frequency and timing for two example catchments in England, using a catchment-based rainfall-runoff model. A nationwide analysis of changes in flood frequency is also presented for one of the transient climate projections, using a grid-based runoff and routing model over the UK. Section 2 describes the regional climate model data, the hydrological models, and the catchments modelled. The results are presented in Section 3 and discussed in Section 4.

# 2. Data, models and methods

## 2.1 Regional Climate Model data

Climate data are taken from three runs of the Met Office Hadley Centre RCM HadRM3 (~25km resolution over the UK) nested within their HadCM3 global model (Pope *et al.* 2000). The RCM includes the land-surface model MOSES (Cox *et al.* 1999). A perturbed parameter ensemble of this system was produced for UKCP09 (Murphy *et al.* 2009), with each run going from 1 January 1950 to 30 November 2099 (under the A1B emissions scenario; IPCC 2000). The ensemble consists of a run with the standard parameterisation, and ten runs with alternative but equally plausible parameter settings in the global model, with equivalent changes applied in the parameterisation of the RCM. Due to the large amount of data required for long transient runs, rather than time-slice runs, only three of the ensemble members have been applied here; the standard RCM HadRM3Q0 (whose parent GCM is HadCM3Q0, climate sensitivity 3.50K), plus HadRM3Q3, whose parent GCM (HadCM3Q3) has low climate sensitivity (2.52K), and HadRM3Q16, whose parent GCM (HadCM3Q16) has high climate sensitivity (5.46K). Note that the length of an RCM year is only 360 days, comprising of twelve 30-day months.

## 2.2 Hydrological models

The main hydrological model used is the Probability Distributed Model (PDM; Moore 1985, 2007), which is a flexible, conceptual rainfall-runoff model, requiring inputs of catchment-average rainfall and potential evaporation (PE). The model has been widely applied in Britain and a version forms part of the River Flow Forecasting System (Moore *et al.* 2005). The full PDM has a variety of formulations, but a simplified version is used here, to reduce the potential for equifinality and allow automatic calibration via Monte Carlo sampling of the parameter space. The version used has six catchment-specific parameters; three of these require calibration, while a fourth is set using soils data and the remaining two are set according to catchment location. This version, and its automatic calibration method, are refinements of those described by Kay *et al.* (2007). See Crooks *et al.* (2009) for more detail.

A second hydrological model, the Grid-to-Grid (G2G; Bell *et al.* 2007, Bell *et al.* 2009), is used for the nationwide analysis of changes in flood frequency, to demonstrate the range of impacts across the UK. This is a grid-based runoff and routing model, which requires rainfall and PE data on a 1km grid over the UK. Recent enhancements to the G2G (Bell *et al.* 2009), involving the use of digital soil datasets for model configuration, resulted in relatively good model performance for a wide range of catchments across Britain.

### 2.3 Input of RCM data to the hydrological models

Precipitation, at an hourly time-step, is a direct output of the RCM, and just has to be converted into catchment average rainfall for input to the PDM. Standard average annual rainfall (SAAR) data are used for this, along with area-weighting, following the method of Kay *et al.* (2006b). For G2G, a similar method is used to downscale the rainfall data to the 1km grid (Bell *et al.* 2007). Note that SAAR data are used simply to confer greater spatial structure on the RCM precipitation data, rather than being any form of bias-correction.

PE from a vegetated surface is not a direct output of the RCM, and thus has to be produced from other RCM variables. Previously this was done using fixed literature values of canopy resistance for short grass along with meteorological variables (Kay *et al.* 2006b), using the Penman-Monteith equation (Monteith 1965). Recently a new method was developed which estimates Penman-Monteith PE using time-varying values of canopy resistance produced by an RCM with an embedded land-surface scheme (Bell *et al.* 2011). PE produced in this way is comparable to observation-based PE from MORECS (Meteorological Office Rainfall and Evaporation Calculation System; Thompson *et al.* 1982; Hough *et al.* 1996). As canopy resistance depends on the level of $CO_2$ in the atmosphere, the inclusion of this mechanism of change in PE could be important for more accurate projections of future flows. Thus vegetated-surface PE was produced for each RCM grid square, then a catchment average PE is produced using simple area-weighting (Kay *et al.* 2006b), for input to the PDM. For G2G, each 1km point simply uses the PE from its corresponding RCM grid square.

### 2.4 Catchments

The two example catchments are the Beult at Stile Bridge (National River Flow Archive catchment number 40005; see www.ceh.ac.uk/data/nrfa/), and the Duddon at Duddon Hall (catchment number 74001), in south-east and north-west England respectively. The catchment locations are shown on the map in Figure 1, and some details of the catchments are given in Table 1. Both catchments are essentially rural, but are very different in terms of area, topography and current rainfall / water balance regime. These

Figure 1
Table 1

factors, as well as location (amongst other things), mean a differing impact of climate change. Concurrent hourly flow and rainfall data (and monthly PE data) are available for PDM calibration for the period 1985-2001. The PDM is then run at an hourly time-step with the alternative RCM-derived input data for each catchment.

Figure 2 shows the RCM-derived catchment-average precipitation and PE for the two catchments, cumulated over the full 149 years, both annually and for each season separately (Spring – March-May; Summer – June-August; Autumn – September-November; Winter – December-February). These demonstrate the differing climatology of the two catchments, with precipitation always exceeding PE for the Duddon, but summer PE exceeding precipitation for the Beult. They also show differences between the three RCM ensemble members, with HadRM3Q3 generally having the highest PE for both catchments, but HadRM3Q0 having the highest rainfall for the Beult and HadRM3Q16 having the highest rainfall for the Duddon. Note that both catchments are smaller in area than the size of one RCM grid square, but include parts of more than one grid square.

Figure 2

## 2.5 Annual maxima and flood frequency

To investigate the changes in flood frequency and timing through the period, annual maxima (AM) are extracted from the modelled flow time-series (for water years, 1st October – 30th September, rather than calendar years). Thus 149 AM are saved, with their date of occurrence, for each run, with the period 1st January – 30th September 1950 used as a run-in period. This is done for the flows at the hourly time-step, as output by the hydrological model, and for daily-mean and (running) 30-day mean flows. The date of occurrence kept with the AM from the 30-day mean flows is that in the middle of the 30 days. The aim of looking at daily and 30-day mean flows as well as hourly flows, even on these relatively small catchments, is to investigate if the projected changes in rainfall may have differential effects on flows at different durations.

The change in flood frequency is then investigated by fitting a flood frequency curve to the data values in a moving window through each 149-year AM time-series. The length of the window is fixed at 30 years, thus 120 flood frequency curves are fitted for each AM time-series. This 30-year time-slice length is standard for climate studies (e.g. UKCP09, Murphy *et al.* 2009), as it is generally considered sufficiently long to represent an average climate yet not too long that any climate change over the period begins to dominate. A generalised logistic (GLO) distribution (Eq. 1) is applied to fit the flood frequency curves, as this is recommended for UK catchments (Robson and Reed 1999), and is fitted using L-moments. This method assumes stationarity over the (30-year) data period, and the fitted curve should not be used for extrapolation to return periods much beyond the length of the data period.

Plots and trend analyses are then performed on the derived time-series, either of flood peaks with a specific return period (e.g. $T$=2, 10 and 50 years), or of the parameters of the fitted GLO distribution (the location $\xi$, scale $\alpha$ and shape $k$; Eq. 1).

$$Q_T = \xi + (\alpha / k) \left( 1 - (T - 1)^{-k} \right) \qquad (k \neq 0) \qquad (1)$$

Note that the value of the GLO location parameter $\xi$ is equivalent to the flood peak with a 2-year return period. An increase in the location parameter $\xi$ has the effect of shifting the whole flood frequency curve upwards, while an increase in the scale parameter $\alpha$ causes a greater increase at higher return periods than at lower return periods (with no change at the 2-year return period). A positive value of the shape parameter $k$ represents a curve that is bounded above (by $\xi+\alpha/k$) as $T\rightarrow\infty$, while a curve with negative $k$ is not bounded above (but is bounded below). A decrease in an already negative value of the shape parameter $k$ thus results in a significant increase in flood peaks at higher return periods. Note that the results presented here for the 50-year return period represent a slight extrapolation of the fitted flood frequency curve, given the 30-year moving window length, and thus contain greater uncertainty than the results for lower return periods.

The change in flood timing is investigated by converting the date of occurrence of each AM into $(r,\theta)$ coordinates, where $r$ is the year number (the Oct 1950 – Sep 1951 AM being year number 1) and $\theta$ is the day number (with 1st January being day number 1, 1st February day number 31 etc., remembering that the RCM has 360-day years). The AM dates can then be plotted on circular plots, and circular statistics used to calculate the mean date of occurrence in a 30-year moving window, as used for the flood frequency analysis above. The use of peaks-over-threshold (POT) would provide more information than AM, particularly about flood timing. However, the extraction of POT presents practical problems when combined with the moving-window analysis, due to the need to define a threshold for peak extraction. That is, either the threshold is fixed for all windows, in which case there will be more peaks in some windows than others, or the threshold is allowed to vary with the window, in which case a given 'peak' may be treated as such for one position of the window but not for another, despite being located within both windows. Thus, for simplicity, AM have been used here.

## 2.6 Trend analysis and significance testing

The aim of the analysis here is to assess the apparent changes in the peak flow series derived from the RCM ensemble members. Only a single realisation is available for each parameter setting in the global model and this means that there is only a single realisation of the corresponding flows. If other equivalent realisations (that is, an ensemble exploring natural variability, often termed an 'initial condition ensemble') had been available it would have been possible to make stronger conclusions about the behaviour of trends in the flow series (cf. Kendon *et al.* 2008). As it is, there is only the single realisation from which to judge whether there is enough evidence to conclude that the trend, or the apparent direction of any trend, would be reproduced in the general behaviour of other realisations for the same parameter settings. The problem is then essentially equivalent to the statistical assessment of trends in an observed data series, where there is again only a single realisation available.

A trend analysis is performed on each derived time-series of flood peaks, GLO parameters and mean AM dates. As the trends are generally non-linear, isotonic regression (Barlow *et al.* 1972) is applied to fit the best non-decreasing (or non-increasing) step-function to the time-series (implemented via the AMALGM algorithm of Cran 1980). The standard deviation (x2) of the fitted step-function is then used as a measure of the size of the non-linear trend, signed to represent the direction of the trend (+ increasing, - decreasing).

The significance of the trends is estimated via permutation tests on the original time-series of AM data. That is, for 10,000 random permutations (resampling without replacement) of the original AM data, the transient flood frequency curves and mean AM dates are calculated, and isotonic regression lines fitted to each of the re-derived time-series. The significance of the trend in the original time-series can then be assessed by comparison of its size with the distribution of sizes derived from the set of permutations. For instance, a trend that is located in the lowest 5% or highest 5% of the distribution is said to be significant at the 10% level, as the test is two-sided. Tests such as this as do not rely on the validity of any particular assumed distribution of annual maxima, or of the derived transient quantities, as the tests are distribution-free. However, there are concerns, discussed below, that this testing procedure may not fully represent the natural variability in observed climate data within the permuted series.

Some examples of derived time-series and their fitted step-functions are shown in Figure 3, in this case for the GLO location parameter $\xi$. In each case, the black line shows the time-series derived from the original AM data series, with the thick grey line showing the step-function fitted to that derived time-series. The dotted lines show time-series derived from 10 random permutations of the original AM data series. Twice the standard deviation is, respectively for cases a)-c), 11.3, 6.5 and 4.0. Case a) is significant at the 1% level and case b) is significant at the 10% level, whilst case c) is not significant even at the 10% level.

Figure 3

The relevance of the permutation test in the present application depends on the validity of the inherent assumption being made: that, under the null of hypothesis of no trend, the AM series arise as statistically independent and identically distributed random quantities. It is generally thought that there is little “carry-over” effect from year-to-year in annual maximum flow series and similarly that the effect on peak flows of medium and long-term variations, such as that of the NAO, will be small (except perhaps on slowly responding catchments) (Hannaford and Marsh 2007; Robson and Reed 1999, Chapter 21). It is of some importance to note that the climate model used to create each ensemble member here has been judged to simulate the broad spatial and temporal characteristics of NAO variability reasonably well (Murphy *et al.* 2009, Section A3.4.1), and thus that the rainfall and flow series, created in turn, would reflect this variability. However, the concern relates to the resampled series from which the distribution of the test statistic is evaluated given a “no trend” scenario. There are several possible approaches to testing for trend that would allow a better representation of a scenario with no trend but reflecting natural variation. A relatively simple approach might be based on a block bootstrap (e.g. Hannaford and Marsh 2006), but this would require investigating the standardisation of the test statistic (studentization), as this is known to have a substantial effect on the performance of the test procedure (Davison and Hinkley 1997). The most straightforward approach would be to use multiple realisations from the GCM, but this would have substantial implications for computational resources. As the formal output of the statistical test is used here only to provide guidance about the strength of apparent trends compared to random variations, the robustness of the formal conclusions is not of great concern. In the comparison of apparent trends across different locations, the output is used as a convenient way of categorising the amount of trend that might be considered important.

# 3. Results

## 3.1 Catchment flood frequency results

The AM and the transient flood peaks (using a 30-year moving window) at three return periods (2, 10 and 50 years) are shown in Figure 4 for each of the two example catchments (for each of the three RCM ensemble members and three time-steps). These plots demonstrate the presence of natural variability and influence of individual events, particularly for the higher return periods where a higher AM coming into and then out of the moving window can have a large affect on the fitted flood frequency curve. This shows how a standard analysis based on time-slices (e.g. centred on the 1970s and 2080s) could be misleading, as a slight shift in the location of either the baseline or future time-slice could lead to a big difference in the modelled change between those time-slices.

Figure 4

The corresponding transient GLO parameters are shown in Figure 5. These plots indicate that the trends in flood frequency over the 150-year period are often far from linear, and can vary significantly not just by catchment but by RCM ensemble member and by the time-step of the flows analysed. Also, the location parameter contains less of the noise of natural variability than either the scale or shape parameters, as it is based on the lower return period flows which contain less sampling uncertainty.

Figure 5

Table 2 gives the sizes of the trends fitted to each transient series, and indicates their significance as determined by permutation tests. This shows that the Duddon has more significant trends than the Beult, as every one of the nine cases (three time-steps for each of three ensemble members) is significant at least at the 5% level for the 2- and 10-year return periods (with four of the nine still being significant at least at the 10% level for the 50-year return period). For the Beult only the 3 HadRM3Q16 cases are significant at least at the 10% level for the 2- and 10-year return periods (with the hourly flows under HadRM3Q0 also significant at the 10% level at the 2-year return period). However, both catchments have a case that is significant at the 1% level for all three return periods. This is HadRM3Q16 for daily mean flows for the Duddon, and HadRM3Q16 for 30-day mean flows for the Beult. High (low) significance at higher return periods does not necessarily translate into high (low) significance for the higher order GLO parameter though, as for the Duddon it is actually the case of HadRM3Q0 for 30-day mean flows which is significant at the 1% level for all three GLO parameters, whereas the case of HadRM3Q16 with daily mean flows is not significant for the scale or shape parameters. For the Beult, the case of HadRM3Q16 for hourly flows is significant at the 5% level for the shape parameter, and the other two HadRM3Q16 cases are not significant for the shape parameter but significant for the scale parameter.

Table 2

## 3.2 Nationwide flood frequency results

In order to get an idea of the spatial variation in flood frequency trends across the UK, the G2G hydrological model was driven with data from RCM ensemble member HadRM3Q0. The AM were extracted from the simulated daily mean flows for each river point on the 1km grid, and flood frequency curves fitted to a 30-year moving window through the AM series. The same trend analysis as described in Section 2.6 was then performed for each derived time-series. The results for the GLO location and scale parameters ($\xi$ and $\alpha$) are shown in Figure 6, standardised by expressing as a percentage

Figure 6

of an estimate of current QMED (the median annual maximum flood) at each point. The QMED estimates are derived via Flood Estimation Handbook formulae (Morris 2003). Note that the trends (between 1950 and 2099) are expressed as a percentage of current QMED only for reasons of standardisation; the stated percentages are not the changes that can be expected between now and 2099. Also, there may be some slight skewing of the standardised trend for smaller catchments, due to the use of a QMED based on instantaneous flows with trends based on daily mean flows. The trend sizes have been greyed out if they are not significant at the 10% level (using permutation tests). The results for the GLO shape parameter *k* are not shown as they are not significant for much of the country (over 85%).

Figure 6 shows significant positive trends in the location parameter ξ for much of the country, with many places having increases greater than 10% of current QMED. A small number of places, particularly concentrated in northern part of East Anglia and in the upper Thames, have increases in excess of 20% of current QMED. Negative trends, present in a small number of places, are not significant at the 10% level (and are thus greyed out). For the scale parameter α, there are fewer places with significant trends. Where significant, the trend in α is generally positive, although mostly less than 5% of current QMED. However, any positive trend in α is adding (above the 2-year return period) to the increases in flood peaks already suggested by the positive trend in the location parameter ξ, and so could be important for flood management strategy. In particular, some of the same areas that had larger trends in the location parameter (e.g. East Anglia) also seem to have larger trends in the scale parameter (greater than 10% of current QMED), thus further accentuating the potential problem in those areas. A very small number of places have significant negative trends in α, although these are mostly less than 5% of current QMED. There are a lot more places, mainly in Northern Ireland and Scotland, with negative trends in α that are not significant at the 10% level (and thus greyed out), again mostly less than 5% of current QMED.

By extracting the trend sizes and significance values from the G2G results for the two points closest to representing the outlets of the two PDM example catchments, the G2G results can be compared to the corresponding PDM results (for daily mean flows under HadRM3Q0; Table 3). Each of the G2G-based trends is in the same direction as the corresponding PDM trend, and generally has a larger magnitude. The exception is the GLO shape parameter *k* for the Beult, where the G2G-based trend is of slightly smaller magnitude than the PDM trend (although both are negative). The G2G-based trends also show greater significance than the corresponding PDM-based trends. The reasons for the overall differences between the PDM and G2G-based results are unclear, although G2G's simulation of a very high AM in the 1990s for the Beult is the cause of the lower magnitude trend in the GLO shape parameter *k*. One possible reason for the differences could be the G2G's use of spatially-distributed rainfall versus the PDM's use of catchment-average rainfall, and G2G's use of spatially-distributed information on soil depths. This comparison indicates the existence of uncertainty in the results due to hydrological model structure.

Table 3

### 3.3 Timing of AM

Figure 7 shows circular plots of the date of AM occurrence in each of the 149 water years. The day of occurrence within the year is plotted as the angle (anti-clockwise from January on the right to June/July on the left, and back to December), with the water year

Figure 7
Table 4

1950-51 plotted closest to the centre and the water year 2098-99 plotted closest to the outermost circle. The lines show the running mean in a 30-year moving window. These clearly show the difference in seasonality of flooding between the two catchments, and the differing (often highly non-linear) trends in seasonality under the three RCM ensemble members and for flows at different time-steps. It should be noted that a snowmelt module has not been applied in the modelling presented here. Snow processes are probably not a major factor for these two catchments, although they could well affect the trends in AM timing in some parts of Britain.

Table 4 shows the results of the trend analysis performed on the 30-year running mean of the AM dates, with the approximate size of the trend given in terms of the number of days (for the 360-day RCM year), and their significance as determined by permutation tests. This shows that only the Beult has a case significant at the 1% level; for 30-day mean flows under HadRM3Q16. The case of hourly flows under HadRM3Q16 is significant at the 10% level, with the other seven cases for the Beult not significant. The Duddon only has two cases significant at the 10% level; HadRM3Q16 for hourly flows and HadRM3Q0 for daily mean flows. Thus there seems to be very little consistency in terms of which time-steps are more or less likely to have significant trends, either in terms of the mean date of AM occurrence here or the flood peaks in Section 3.1. However, use of HadRM3Q3 is perhaps less likely to result in any significant trends, while use of HadRM3Q16 is perhaps more likely to result in significant trends.

# 4. Discussion

Modelling has been performed for two catchments, using a three-member RCM ensemble for the period 1950-2099. Time-series of AM have been extracted and analysed in terms of flood frequency (using a fitted GLO distribution) and timing in a 30-year moving window. The results suggest that changes are unlikely to occur linearly over the coming century, partly because of the presence of natural variability (the directional effect of which cannot yet be predicted for any given period), but also perhaps due to the inherent non-linear response of hydrological systems. The potential for a large change in flood frequency to occur over a relatively short period of time is something that policy makers need to consider; whether that change is caused by climate change or medium-term natural variability is somewhat immaterial, although it could affect decisions on what type of flood management option to implement. The application of an initial condition ensemble of RCM data, rather than the perturbed parameter ensemble applied here, would help to separate the effects of climate change and natural variability (Kendon *et al.* 2008), and to identify the range of natural variability and perhaps changes in natural variability under climate change.

Non-linear trend analyses performed on derived time-series of flood peak and timing data suggest that perhaps use of the HadRM3Q3 RCM ensemble member is less likely to result in significant flood trends than use of HadRM3Q0, with use of HadRM3Q16 perhaps more likely to result in significant flood trends than use of HadRM3Q0. This is consistent with the relative climate sensitivity of the three ensemble members (Section 2.1). Each of these ensemble members (and the other eight that form the 11-member RCM ensemble used for UKCP09) are considered equally likely (Murphy *et al.* 2009), demonstrating the presence of uncertainty due to climate model parameterization. The full range of climate model uncertainty is likely to be larger than represented here, as these results only represent one GCM, albeit as a perturbed parameter ensemble. Previous research has suggested than GCM structure uncertainty is likely to be the largest source of uncertainty for the hydrological impacts of climate change (Kay *et al.* 2009, Prudhomme and Davies 2009, Graham *et al.* 2007a, b).

The catchment-based (PDM) results suggest greater significance of trends in north-west England than in south-east England. However, there appears to be little consistency in terms of which flow time-steps are more or less likely to have significant trends. This makes detection of changes in flows more complicated as it could differ between catchments not just because of catchment location (due to spatial variation in climate change) but also according to physical catchment characteristics and how these interact with the climatic changes. Detection of changes in modelled extreme rainfall over the UK has been shown to depend on location, duration, extremity and season, with the earliest detection times found in South-West England for 10-day winter precipitation totals with a 10-year return period (Fowler and Wilby 2010).

A nationwide analysis using daily mean flows from the G2G model with HadRM3Q0 RCM data showed that the modelled trends in GLO parameters vary considerably in size across the country. However, all significant trends in the location parameter $\xi$, and almost all significant trends in the scale parameter $\alpha$, are positive, suggesting increased flood risk across much of the country. The areas of significant trends are broadly consistent with the results from an analysis of high flow and flood trends from observed flows in a set of undisturbed catchments in the UK (Hannaford and Marsh 2007). However, this does not mean that trends should already be detectable in observed flows in all of these regions: The modelling here involves much longer time-series than are generally available for flow observations, and the analysis of trends in observed flows is confounded not just by natural climatic variability but by other factors such as land-use change, channel modifications and changes in measurement practises (Wilby *et al.* 2008, Robson 2002).

A comparison of the catchment-based (PDM) results with those from the corresponding locations in G2G showed the presence of hydrological modelling uncertainty, as the G2G-based trends were generally of a larger magnitude (and often more statistically significant) than the corresponding PDM-based trends. Reassuringly though, the directions of the trends in each case were the same. In addition to hydrological model structure uncertainty, there is also uncertainty due to model parameters. However, a number of studies have suggested that uncertainty due to hydrological modelling is smaller than that from the climate modelling (Wilby and Harris 2006, Kay *et al.* 2009, Prudhomme and Davies 2009).

The nationwide (G2G) results and the catchment (PDM) results should be treated with some caution, as in addition to the presence of hydrological model uncertainty neither model includes snowfall and snowmelt. This could significantly alter results in Scotland and north-east England in particular, but runoff for most catchments in Britain is likely to have been affected by snowmelt to some extent, at some time in the recent past. Indeed, the snowmelt-generated flood of March 1947 affected much of the country. Future work will investigate the inclusion of a simple snowmelt module.

# Acknowledgements
Thanks to the UK Met Office Hadley Centre for providing the RCM data.


# References


Barlow, R. E., Bartholomew, D.J., Bremner, J. M. and Brunk, H. D. (1972). Statistical inference under order restrictions; the theory and application of isotonic regression. Wiley, New York

Bell, V.A, Gedney, N., Kay, A.L., Smith, R., Jones, R.G. and Moore, R.J. (2011). Estimating potential evaporation from vegetated surfaces for water management impact assessments using climate model output. Journal of Hydrometeorology.

Bell, V.A., Kay, A.L., Jones, R.G. and Moore, R.J. (2007). Development of a high resolution grid-based river flow model for use with regional climate model output. Hydrology and Earth System Sciences, **11**, 532-549.

Bell, V.A., Kay, A.L., Jones, R.G., Moore, R.J. and Reynard, N.S. (2009). Use of soil data in a grid-based hydrological model to estimate spatial variation in changing flood risk across the UK. Journal of Hydrology, **377**, 335-350.

Cox, P.M., Betts, R.A., Bunton C.B., Essery, R.M., Rowntree, P.R. and Smith, J. (1999). The impact of new land surface physics on the GCM simulation of climate and climate sensitivity. Climate Dynamics, **15,** 183-203.

Cran, G.W. (1980). Amalgamation of Means in the Case of Simple Ordering. Applied Statistics, **29**(2), 209-211.

Crooks, S.M., Kay, A.L. and Reynard, N.S. (2009). Regionalised impacts of climate change on flood flows: hydrological models, catchments and calibration. Report to Department for Environment, Food and Rural Affairs, FD2020 milestone report, CEH Wallingford, November 2009, 53pp.

Davison, A.C. and Hinkley, D.V. (1997). Bootstrap Methods and their Application. Cambridge University Press, Cambridge.

Dettinger, M.D., Cayan, D.R., Meyer, M.K. and Jeton, A.E. (2004). Simulated hydrologic responses to climate variations and change in the Merced, Carson, and American river basins, Sierra Nevada, California, 1900-2099. Climatic Change, **62**, 283-317.

Fowler, H.J. and Kilsby, C.G. (2003). A regional frequency analysis of United Kingdom extreme rainfall from 1961 to 2000. International Journal of Climatology, **23**, 1313-1334.

Fowler, H.J. and Kilsby, C.G. (2007). Using regional climate model data to simulate historical and future river flows in northwest England. Climatic Change, **80**, 337-367.

Fowler, H.J. and Wilby, R.L. (2010). Detecting changes in seasonal precipitation extremes using regional climate model projections: Implications for managing fluvial flood risk. Water Resources Research, **46**, W03525, doi:10.1029/2008WR007636.

Graham, L.P., Andreasson, J. and Carlsson, B. (2007a). Assessing climate change impacts on hydrology from an ensemble of regional climate models, model scales and linking methods — a case study on the Lule River basin. Climatic Change, **81**, 293-307.

Graham, L.P., Hageman, S., Jaun, S. and Beniston, M. (2007b). On interpreting hydrological change from regional climate models. Climatic Change, **81**, 97-122.

Hannaford, J., Laize, C.R. and Marsh, T. (2007). An assessment of runoff trends in natural catchments in the Celtic regions of North West Europe. In: Lobo Ferreira, J.P.; Viera, J.M.P, (eds.) Water in Celtic countries: quantity, quality and climate variability. Proceedings of the Fourth InterCeltic Colloquium on hydrology and management of water resources, Guimaraes, Portugal, 2005. Wallingford, IAHS Press, 78-85. (IAHS Red Book, 310)

Hannaford, J. and Marsh, T.J. (2006). An assessment of trends in UK runoff and low flows using a network of undisturbed catchments. Int. J. Climatology, **26**(9), 1237-1253.

Hannaford, J. and Marsh, T.J. (2007). High-flow and flood trends in a network of undisturbed catchments in the UK. Int. J. Climatology, **28**(10), 1325-1338.

Hough, M., Palmer, S., Weir, A., Lee, M., and Barrie, I. (1996). The Meteorological Office Rainfall and Evaporation Calculation System: MORECS version 2.0 (1995). An update to Hydrological Memorandum 45, The Met. Office, Bracknell.

Hulme, M., Jenkins, G.J., Lu, X.,Turnpenny, J.R., Mitchell, T.D., Jones, R.G., Lowe, J., Murphy, J.M., Hassell, D., Boorman, P., McDonald, R. and Hill, S. (2002). Climate Change Scenarios for the United Kingdom: The UKCIP02 Scientific Report. Tyndall Centre for Climate Change Research, School of Environmental Sciences, University of East Anglia, Norwich, UK.

IPCC (2000). Special report on emissions scenarios (SRES): A special report of Working Group III of the Intergovernmental Panel on Climate Change. Cambridge University Press, Cambridge.

Kay, A.L., Davies, H.N., Bell, V.A. and Jones, R.G. (2009). Comparison of uncertainty sources for climate change impacts: flood frequency in England. Climatic Change, **92**(1-2), 41-63, doi: 10.1007/s10584-008-9471-4.

Kay, A.L., Jones, D.A., Crooks, S.M., Kjeldsen, T.R. and Fung, C.F. (2007). An investigation of site-similarity approaches to generalisation of a rainfall-runoff model. Hydrology and Earth System Sciences, **11**(1), 500-515.

Kay, A.L., Jones, R.G. and Reynard, N.S. (2006a). RCM rainfall for UK flood frequency estimation. II. Climate change results. J. Hydrol. **318**, 163-172.

Kay, A.L., Reynard, N.S. and Jones, R.G., (2006b). RCM rainfall for UK flood frequency estimation. I. Methods and validation. J. Hydrol. **318**, 151-162.

Keenlyside, N.S., Latif, M., Jungclaus, J., Kornblueh, L. and Roeckner, E. (2008). Advancing decadal-scale climate prediction in the North Atlantic sector. Nature, **453**, 84-88.

Kendon, E.J., Rowell, D.P., Jones, R.G. and Buonomo, E. (2008). Robustness of future changes in local precipitation extremes. Journal of Climate, **21**, 4280-4297.

Kerr, R.A. (2007). Humans and nature dual over the next decade's climate. Science, **317**, 746-747.

Kundzewicz, Z.W. and Robson, A.J. (2004). Change detection in hydrological records – a review of the methodology. Hydrol. Sci. J. **49**(1), 7-19.

Monteith, J.L. (1965). Evaporation and environment. Symp. Soc. Exp. Biol. **19**, 205-234.

Moore, R.J. (1985). The probability-distributed principle and runoff production at point and basin scales. Hydrol. Sci. J. **30**(2), 273-297.

Moore. R.J. (2007). The PDM rainfall-runoff model. Hydrol. Earth Syst. Sci. **11**(1), 483-499.

Moore, R.J., Bell, V.A. and Jones, D.A. (2005). Forecasting for flood warning. C.R. Geoscience, **337**, 203-217.

Morris, D.G. (2003). Automation and appraisal of the FEH statistical procedures for flood frequency estimation. Report to UK Department for Environment, Food and Rural Affairs and the Environment Agency, Project FD1603 technical report, CEH Wallingford, October 2003, 207pp.

Murphy, J.M., Sexton, D.M.H., Jenkins, G.J., Booth, B.B.B., Brown, C.C., Clark, R.T., Collins, M., Harris, G.R., Kendon, E.J., Betts, R.A., Brown, S.J., Humphrey, K.A., McCarthy, M.P., McDonald, R.E., Stephens, A., Wallace, C., Warren, R., Wilby, R. and Wood, R.A. (2009). UK Climate Projections Science Report: Climate change projections. Met Office Hadley Centre, Exeter.

Pope V.D., Gallani M.L., Rowntree P.R. and Stratton R.A. (2000). The impact of new physical parametrizations in the Hadley Centre climate model: HadAM3. Climate Dynamics**,** **16**(2-3), 123-146.

Prudhomme, C. and Davies, H.N. (2009). Assessing uncertainties in climate change impact analyses on river flow regimes in the UK. Part 2: future climate. Climatic Change, 93, 197-222, doi: 10.1007/s10584-008-9461-6.

Prudhomme, C., Reynard, N. and Crooks, S. (2002). Downscaling from global climate models for flood frequency analysis: where are we now? Hydrological Processes, **16**, 1137-1150.

Reynard, N.S., Crooks, S.M. and Kay, A.L. (2004). Impact of climate change on flood flows in river catchments. Report to the UK Department for Environment, Food and Rural Affairs and the Environment Agency, Project SC010011 technical report, CEH Wallingford, March 2004, 97pp.

Robson, A.J. (2002). Evidence for trends in UK flooding. Phil. Trans. R. Soc. Lond. A, **360**, 1327-1343, doi:10.1098/rsta.2002.1003.

Robson A.J. and Reed D.W. (1999). Statistical procedures for flood frequency estimation. Vol. 3, Flood Estimation Handbook. Institute of Hydrology, Wallingford, UK, 338pp.

Smith, D.M., Cusack, S., Colman, A.W., Folland, C.K., Harris, G.R. and Murphy, J.M. (2007). Improved surface temperature prediction for the coming decade from a global climate model. Science, **317**, 796-799.

Thodsen, H. (2007). The influence of climate change on stream flow in Danish rivers. Journal of Hydrology, **333**, 226-238.

Thompson, N., Barrie, I.A. and Ayles, M. (1982). The Meteorological Office Rainfall and Evaporation Calculation System: MORECS (July 1981). Hydrological Memorandum No. 45, Met Office, Bracknell.

Wood, R. (2008). Natural ups and downs. Nature, **453**, 43-44.

Wilby, R.L., Beven, K.J. and Reynard, N.S. (2008). Climate change and fluvial flood risk in the UK: more of the same? Hydrological Processes, **22**, 2511-2523.

Wilby R.L. and Harris, I. (2006). A framework for assessing uncertainties in climate change impacts: Low-flow scenarios for the River Thames, UK. Water Resources Research, **42**, W02419, doi:10.1029/2005WR004065.

# Tables and Figures

**Table 1 Details of the example catchments, from the UK National River Flow Archive (NRFA).**

| Catchment name (River @ Location) | NRFA catchment number | Catchment area [$km^2$] | Median altitude (altitude range)[m] | Mean annual rainfall [mm] | Mean annual runoff [mm] |
|---|---|---|---|---|---|
| Beult @ Stile Bridge | 40005 | 277.1 | 39 (12-161) | 706 | 233 |
| Duddon @ Duddon Hall | 74001 | 85.7 | 291 (15-794) | 2218 | 1769 |

**Table 2 Modelled trends in flood frequency for the two example catchments, for the three RCM ensemble members and at three time-steps. Trends are shown for three return periods (2, 10 and 50 years), and in terms of the fitted GLO parameters. The significance of each trend is indicated underneath it (see key at bottom of table).**

| | | Hourly flows | | | Daily mean flows | | | 30-day mean flows | | |
|---|---|---|---|---|---|---|---|---|---|---|
| | | HadRM3 Q0 | HadRM3 Q3 | HadRM3 Q16 | HadRM3 Q0 | HadRM3 Q3 | HadRM3 Q16 | HadRM3 Q0 | HadRM3 Q3 | HadRM3 Q16 |
| Beult (40005) | Return period | | | | | | | | | |
| | 2-year (= location ξ) | 6.5 | 4.0 | 11.3 | 4.5 | 2.5 | 9.2 | 1.0 | 0.8 | 2.8 |
| | | * | - | *** | - | - | *** | - | - | *** |
| | 10-year | 8.8 | 6.8 | 13.5 | 8.3 | 4.4 | 13.5 | 1.6 | 1.4 | 4.5 |
| | | - | - | * | - | - | ** | - | - | *** |
| | 50-year | 15.5 | 6.9 | 16.4 | 20.6 | -10.8 | 18.2 | 3.3 | 1.6 | 6.1 |
| | | - | - | - | - | - | - | ** | - | *** |
| Beult (40005) | GLO parameter | | | | | | | | | |
| | Scale α | 1.04 | 1.93 | 2.20 | 0.87 | 1.47 | 2.54 | 0.28 | 0.38 | 0.75 |
| | | - | - | - | - | - | * | - | - | ** |
| | Shape *k* | -0.09 | 0.09 | 0.20 | -0.16 | 0.11 | 0.16 | -0.13 | 0.11 | 0.06 |
| | | - | - | ** | - | - | - | - | - | - |
| Duddon (74001) | Return period | | | | | | | | | |
| | 2-year (= location ξ) | 20.2 | 14.4 | 23.1 | 7.1 | 7.2 | 13 | 3.3 | 2.1 | 2.7 |
| | | *** | *** | *** | ** | *** | *** | *** | *** | *** |
| | 10-year | 30.9 | 23.9 | 25.1 | 12.5 | 12.9 | 18.1 | 4.1 | 2.2 | 3.4 |
| | | *** | ** | ** | ** | ** | *** | *** | ** | *** |
| | 50-year | 46.5 | 45.5 | 24.2 | 23.6 | 20.9 | 30 | 3.8 | 2.7 | 3.9 |
| | | * | * | - | - | - | *** | * | - | - |
| Duddon (74001) | GLO parameter | | | | | | | | | |
| | Scale α | 4.17 | 2.67 | 2.67 | 1.42 | 2.18 | 1.75 | 0.74 | 0.18 | 0.43 |
| | | - | - | - | - | - | - | *** | - | - |
| | Shape *k* | 0.11 | -0.15 | 0.15 | -0.10 | -0.07 | -0.14 | 0.27 | 0.10 | 0.07 |
| | | - | - | - | - | - | - | *** | - | - |

Key: *** significant at 1% level; ** significant at 5% level; * significant at 10% level; - not significant

**Table 3 Comparison of modelled trends in flood frequency using the PDM and G2G models, for daily mean flows using the HadRM3Q0 ensemble member for the two example catchments. Trends are shown for three return periods (2, 10 and 50 years), and in terms of the fitted GLO parameters. The significance of each trend is indicated underneath it (see key at bottom of table).**

| | Beult (40005) | | Duddon (74001) | |
|---|---|---|---|---|
| | PDM | G2G | PDM | G2G |
| Return period | | | | |
| 2-year | 4.5 | 6.7 | 7.1 | 10.3 |
| (= location ξ) | - | *** | ** | *** |
| 10-year | 8.3 | 13.3 | 12.5 | 19.3 |
| | - | - | ** | *** |
| 50-year | 20.6 | 34.4 | 23.6 | 37.7 |
| | - | - | - | *** |
| GLO parameter | | | | |
| Scale α | 0.87 | 1.65 | 1.42 | 1.88 |
| | - | - | - | - |
| Shape $k$ | -0.16 | -0.14 | -0.10 | -0.19 |
| | - | - | - | * |

Key: *** significant at 1% level; ** significant at 5% level;
* significant at 10% level; - not significant

**Table 4 Modelled trends in the mean date of AM occurrence for the two main example catchments, for the three RCM ensemble members and at three time-steps. Trends are given in terms of the number of days (in the 360-day year of the RCM). The significance of each trend is indicated underneath it (see key at bottom of table).**

| Catchment | Hourly flows | | | Daily mean flows | | | 30-day mean flows | | |
|---|---|---|---|---|---|---|---|---|---|
| | HadRM3 Q0 | HadRM3 Q3 | HadRM3 Q16 | HadRM3 Q0 | HadRM3 Q3 | HadRM3 Q16 | HadRM3 Q0 | HadRM3 Q3 | HadRM3 Q16 |
| Beult | -11.8 | 8.5 | -12.7 | -11.9 | 8.8 | -12.5 | -9.3 | -3.5 | -15.2 |
| (40005) | - | - | * | - | - | - | - | - | *** |
| Duddon | 22.3 | -9.0 | 21.8 | 26.6 | -10.7 | 18.1 | -13.3 | -7.4 | -14.4 |
| (74001) | - | - | * | * | - | - | - | - | - |

Key: *** significant at 1% level; ** significant at 5% level; * significant at 10% level; - not significant

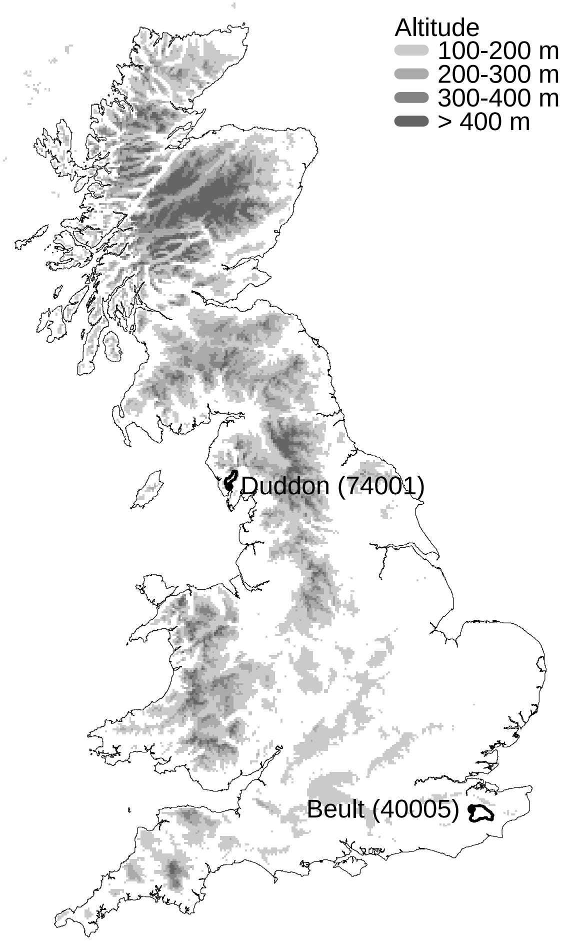


**Figure 1 The locations of the example catchments.**

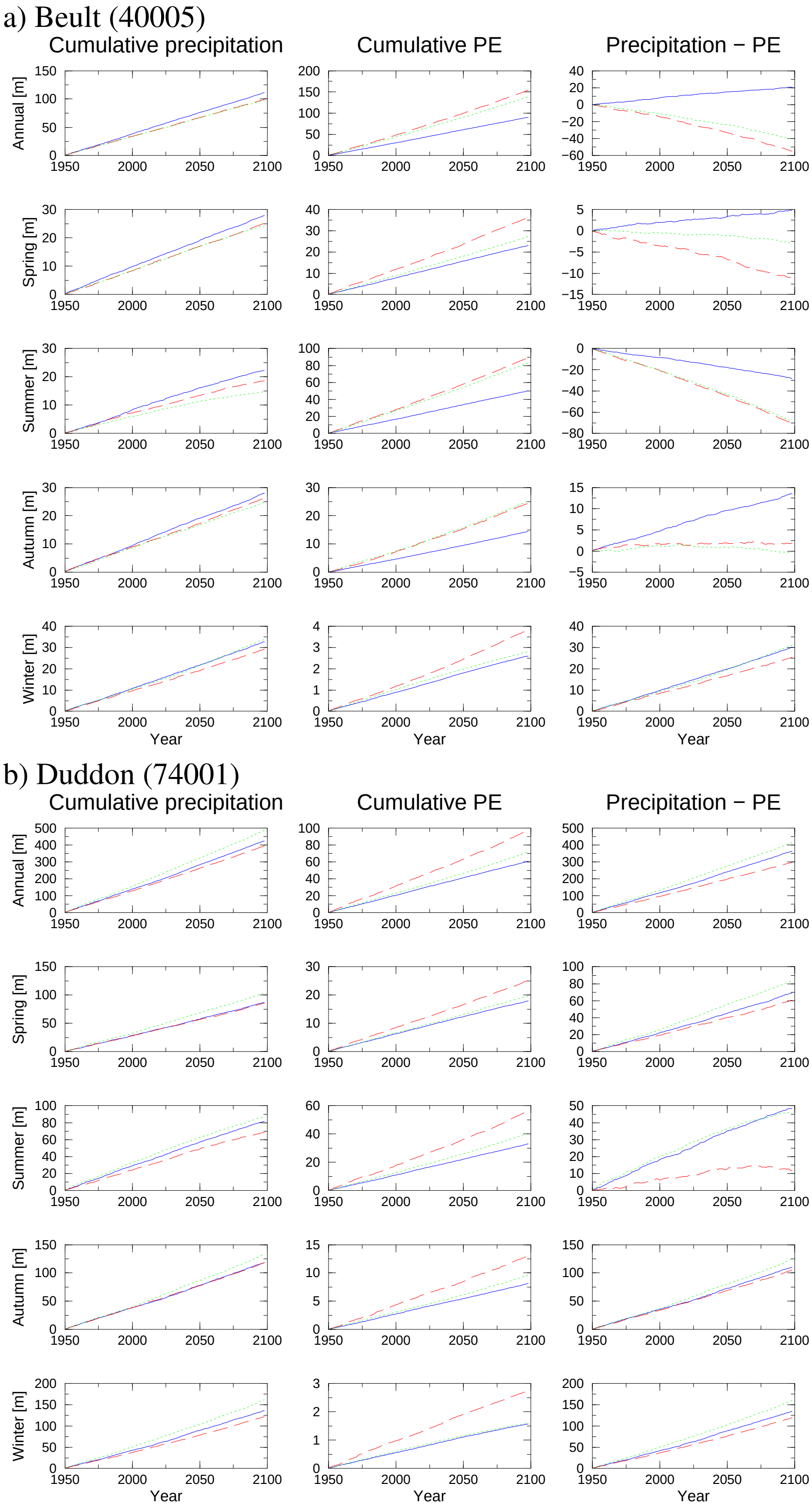


**Figure 2 Cumulative catchment average (annual and seasonal) precipitation and PE (and the difference between the two) for the two example catchments, under each of the RCM ensemble members (HadRM3Q0 – blue solid, HadRM3Q3 – red dashed, HadRM3Q16 – green dotted).**

a)
b)
c)
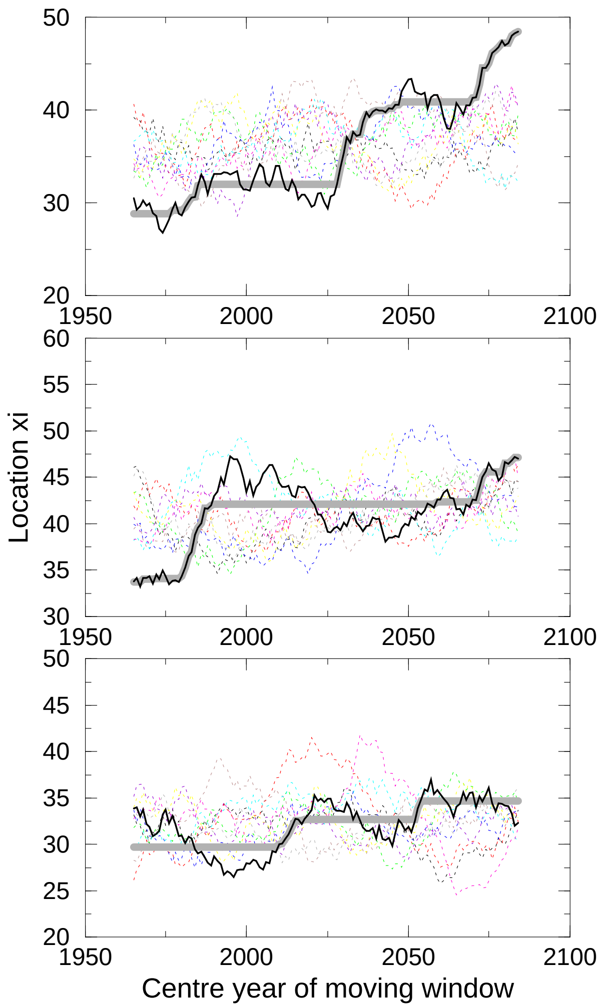


**Figure 3 Examples of derived time-series (black solid lines) and their fitted step-functions (thick grey lines), along with time-series derived from permutations of the original data (dotted lines).**

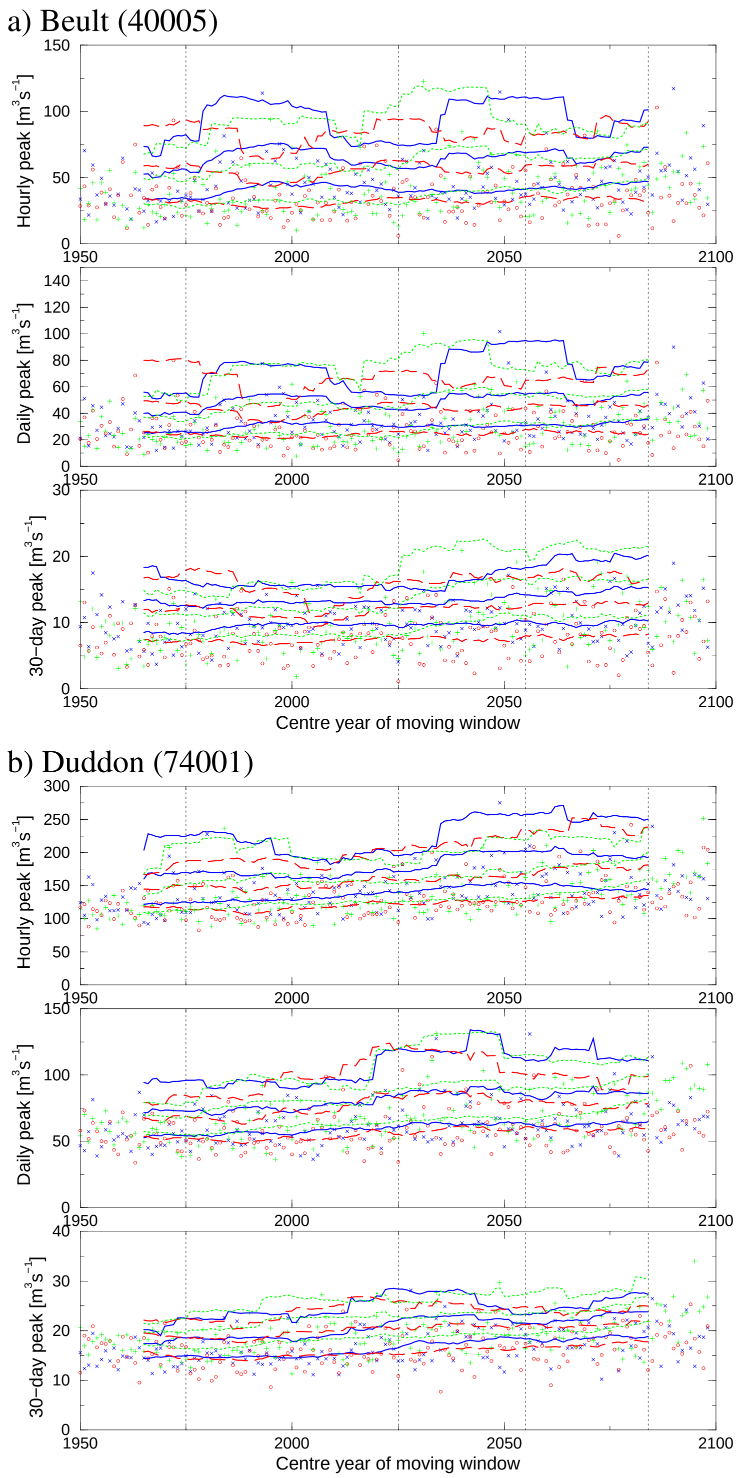


**Figure 4 Simulated AM, and transient flood peaks at three return periods (2, 10 and 50 years), for the two example catchments, under each of the RCM ensemble members (HadRM3Q0 – blue crosses / solid lines, HadRM3Q3 – red circles / dashed lines, HadRM3Q16 – green plus signs / dotted lines). The transient flood peaks are derived from fitting a flood frequency curve to the AM in a 30-year moving window. The vertical dotted lines represent the positions of the standard 30-year time-slices (1970s, 2020s, 2050s and 2080s).**

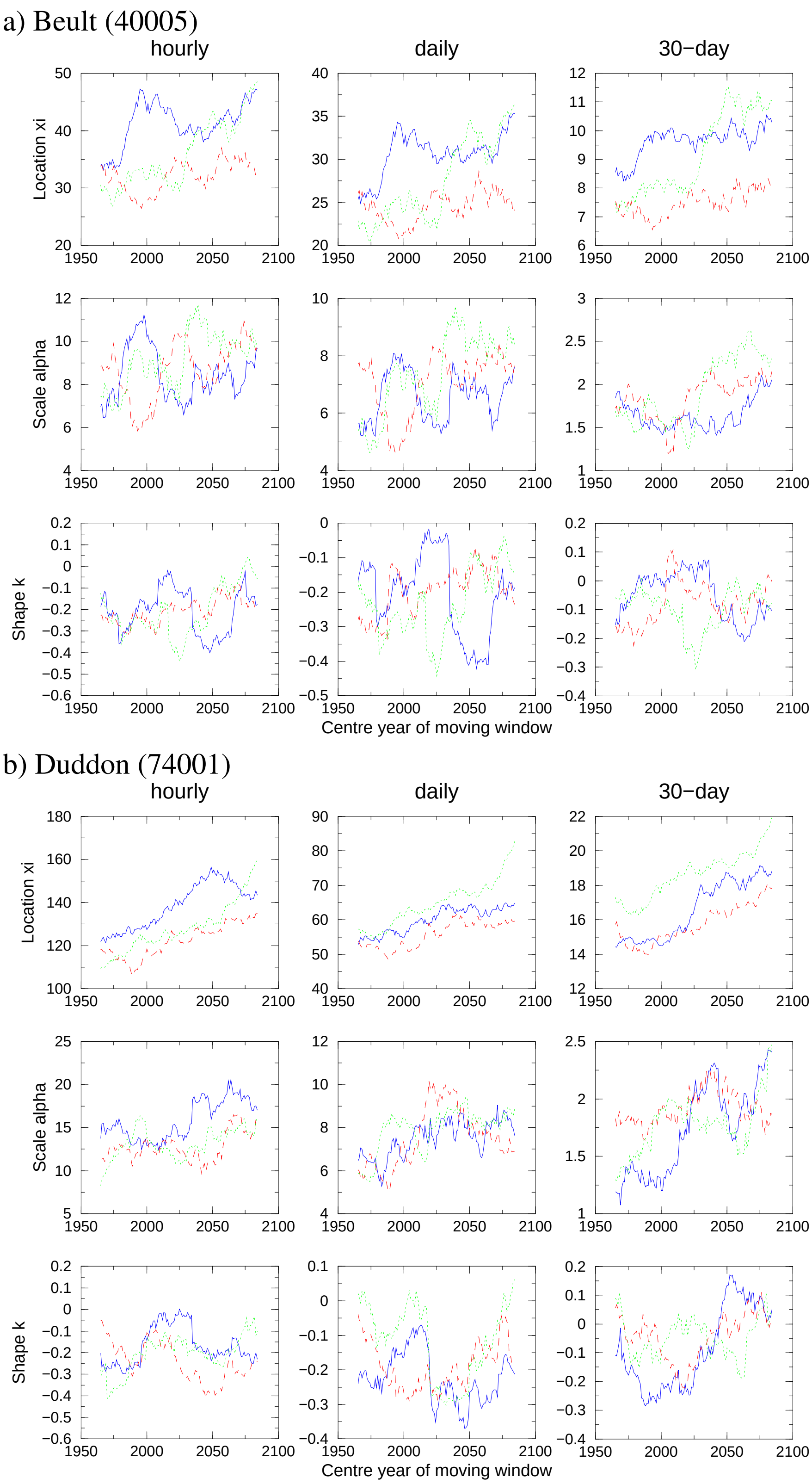


**Figure 5 The transient GLO parameters under each of the RCM ensemble members (HadRM3Q0 – solid blue, HadRM3Q3 – dashed red, HadRM3Q16 – dotted green), for the two example catchments.**

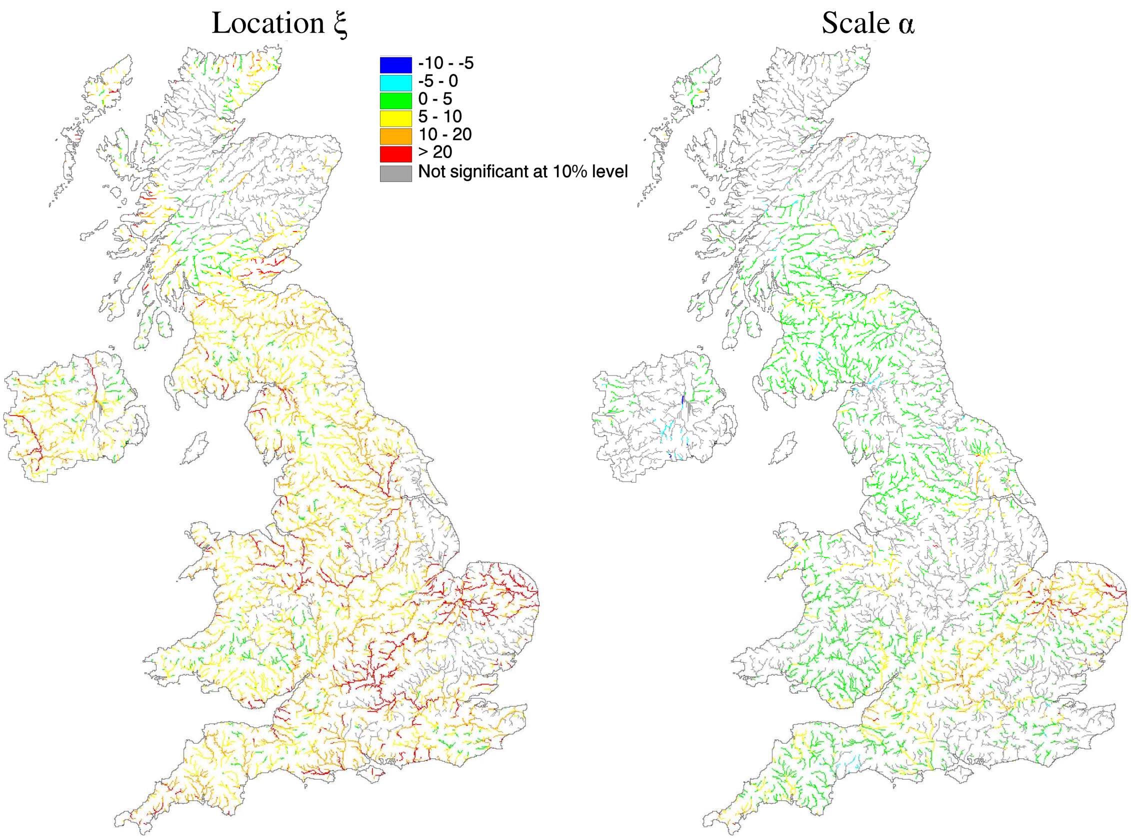


**Figure 6 Nationwide trends in the GLO location and scale parameters (as a percentage of current QMED), from daily mean AM modelled using the G2G hydrological model with HadRM3Q0 RCM data. Trends that are not significant at the 10% level are greyed out.**

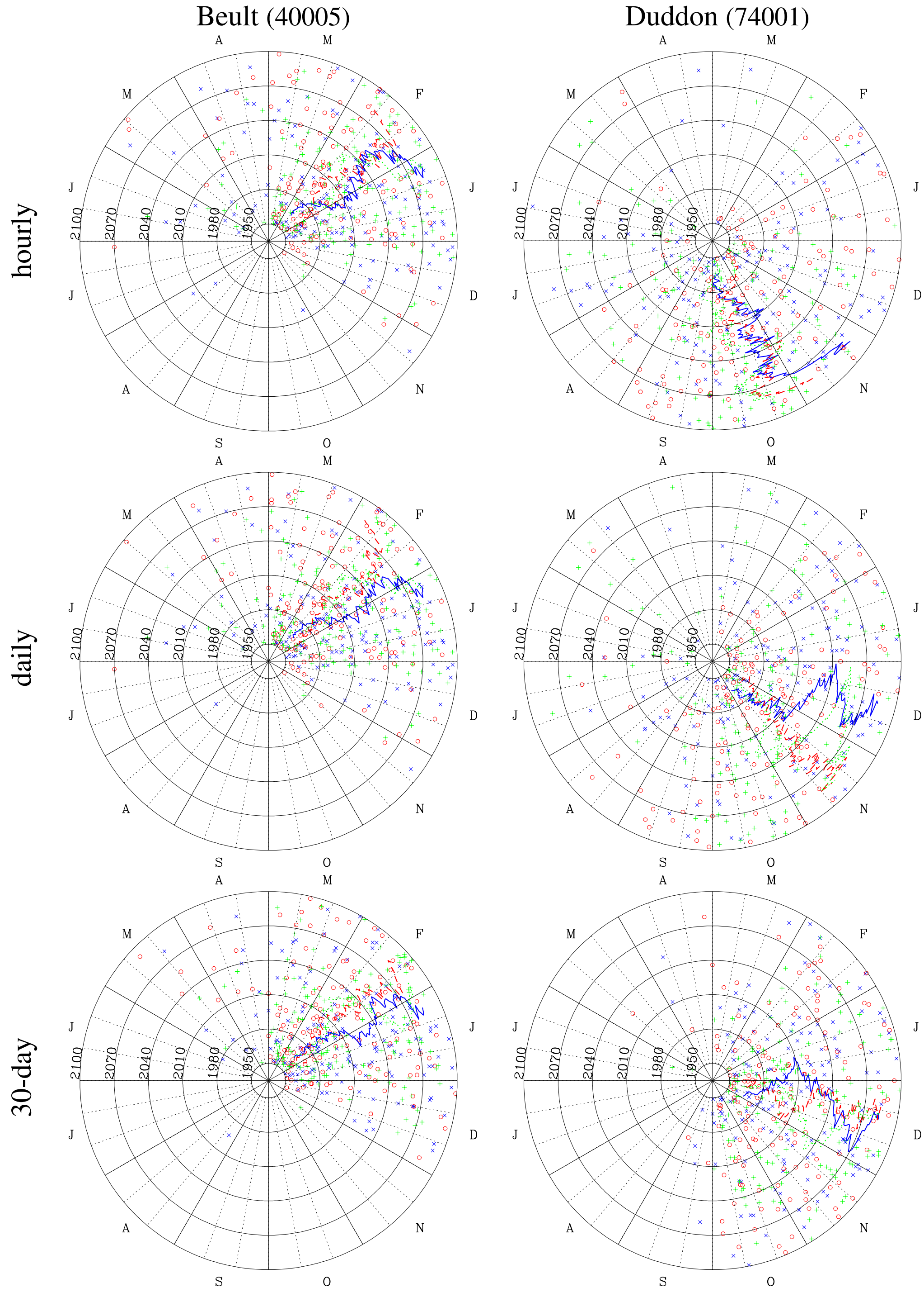


**Figure 7 Circular plots for the two example catchments, showing the date of occurrence of each AM (symbols) with the transient mean in a 30-year moving window (lines), under each of the RCM ensemble members (HadRM3Q0 – blue crosses / solid lines, HadRM3Q3 – red circles / dashed lines, HadRM3Q16 – green plus signs / dotted lines).**